Degree of *N*-Methylation of Nucleosides and Metabolites Controls Binding Affinity to Pristine Silica Surfaces

Mouzhe Xie[1,2]* *and Rafael Brüschweiler*[1,3,4]*

[1] Department of Chemistry and Biochemistry, The Ohio State University, Columbus, Ohio 43212, USA

[2] Current address: Pritzker School of Molecular Engineering, the University of Chicago, Chicago, Illinois 60637, USA

[3] The Campus Chemical Instrument Center, The Ohio State University, Columbus, Ohio 43212, USA

[4] Department of Biological Chemistry and Pharmacology, The Ohio State University, Columbus, Ohio 43212, USA

AUTHOR INFORMATION

Corresponding Authors

* Mouzhe Xie xiemouzhe@uchicago.edu ORCID: 0000-0002-2960-644X

* Rafael Brüschweiler bruschweiler.1@osu.edu ORCID: 0000-0003-3649-4543

ABSTRACT. Biological molecules interact with silica (SiO_2) surfaces with binding affinities that greatly vary depending on their physical chemical properties. However, the quantitative characterization of biological compounds adsorbed on silica surfaces, especially of compounds involved in fast, reversible interactions, has been challenging and the driving forces are not well understood. Here, we show how carbon-13 NMR spin relaxation provides quantitative atomic-detail information about the transient molecular binding to pristine silica surfaces, represented by colloidally dispersed silica nanoparticles (SNPs). Based on the quantitative analysis of almost two dozen biological molecules, we find that the addition of *N*-methyl motifs systematically increases molecular binding affinities to silica in a nearly quantitatively predictable manner. Among the studied compounds are many methylated nucleosides, which is common in epigenetic signaling in nucleic acids. The quantitative understanding of *N*-methylation may open up new ways to detect and separate methylated nucleic acids or even regulate their cellular functions.

TOC GRAPHIC

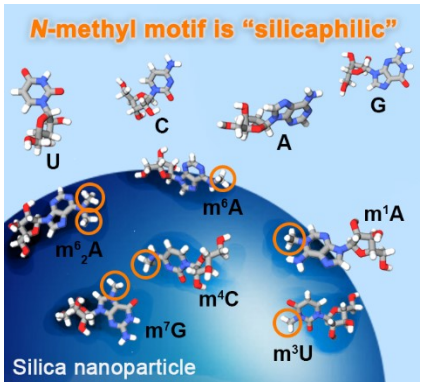

Keywords:

N-methylation, nucleosides, silica-nanoparticles, NMR spin relaxation, quantitative binding affinities, reversible exchange

Deciphering molecular adsorption to silica surfaces is key to the better understanding of numerous phenomena and processes encountered in basic research and industry, such as bioanalysis,[1] chromatography,[2] heterogenous catalysis,[3] contamination control,[4] biomedical engineering,[5] and targeted drug delivery.[6] Pristine silica surfaces display both siloxane (Si–O–Si) and silanol (Si–OH) groups, whereby the latter undergo partial deprotonation at (near-)neutral pH, leading to an overall negative surface charge.[7] Experimental and computational studies have identified several physical-chemical determinants of molecule-silica interactions. For example, positively charged molecules often possess increased affinity for pristine (negatively charged) silica surfaces via electrostatic attraction, but other interactions, such as hydrogen bonding, van der Waals forces, and hydrophobic effects, can also make significant contributions to molecular adsorption.[8-11]

Current knowledge is still limited and far from being able to explain or predict the molecular adsorption behavior of many kinds of molecules. Existing methods often do not provide quantitative binding properties and atomic resolution information or they only report on a small subset of molecules with specific optical or chemical properties. Most methods are best suited to study strong interactions, sometimes under harsh conditions (e.g. isothermal titration calorimetry,[12] electron microscopy,[13] and X-ray absorption[14]), but less so for weak, reversible, and highly dynamic interactions with K_D's in the sub-mM and μM range. These weaker reversible interactions can be highly relevant in practice.[15] Several recent solution NMR-based studies have provided useful new insights using translational diffusion filtering, relaxation dispersion, or saturation transfer experiments.[16-18] Most previous studies focused on relatively few compounds, such as water, ethanol, NO, CO_2, benzene, pyridines, and some of the naturally occurring amino acids.[19-24] By contrast, very little is known about the binding properties of many

other biological compounds, including metabolites and building blocks of biomacromolecules that play key roles in biology. Such incomplete coverage has prevented the broader understanding of specific driving forces of molecule-silica interactions.[25]

We recently demonstrated that silica nanoparticles (SNPs) can substantially affect NMR signals of certain metabolite molecules in solution, which was utilized to assist the characterization of complex metabolomics mixtures.[26] These effects are caused by transient interactions of metabolites with the much larger and, hence, much more slowly tumbling nanoparticles. It leads to the retardation of the rotational tumbling of the interacting metabolites and thereby expedites their transverse spin relaxation, but without affecting the NMR peak positions. This causes NMR line broadening or even to the complete disappearance of resonances allowing molecule-specific identification and quantification of molecule-nanoparticle interactions. When applying this SNP-assisted NMR method to human urine, as an example of a complex mixture consisting of several hundred different metabolites, positively charged metabolites that interact with SNPs via electrostatic attraction could be readily identified. Interestingly, certain neutral metabolites also showed interactions with SNPs, in particular metabolites with an amine carrying one or several methyl groups. Metabolites that contained this type of "*N*-methyl motif" included carnitine, 1-methylhistidine, and trigonelline.[26] In another NMR-based metabolomics study, two other *N*-methyl carrying molecules were identified, namely choline and creatinine, because of their strong interactions with silica surfaces leading to irreversible adsorption.[27] These qualitative observations suggest a silicaphilic nature of *N*-methyl group-containing molecules, a phenomenon that hitherto has not been systematically and quantitatively investigated and which is the subject of this work.

N-methyl motifs are also common in naturally occurring nucleic acids.[28-29] In cells, both DNA and RNA can be enzymatically methylated and de-methylated enabling control of the flow of genetic information by epigenetic modifications.[30-31] Common forms of methylation in nucleic acids are N^6-methyladenosine,[32] 5-methylcytosine,[33] N^6,N^6-dimethyladenosine,[34] N^7-methylguanosine,[35] and N^1-methyladenosine,[36] many of which involve one or several *N*-methyl motifs that are germane to the current study. Considering the important biological functions of nucleic acid methylation, a central question is: what physical-chemical properties determine their function, for example, for specific enzyme recognition?[37] A recent study suggested that the subtle change in polarity and hydrophobicity may play a crucial role in the molecular recognition of N^6-methylated adenine by its protein binding partner, the YTH domain, through a non-covalent interaction described as an "aromatic cage".[38] In order to obtain a mechanistic understanding of these processes, sensitive and quantitative experimental approaches are needed that are capable of detecting the effect of methylation on nucleic acid interactions.

In this letter, we utilize high-resolution solution NMR to quantitatively study the molecular adsorption behavior before and after methylation to pristine silica surfaces. The SNPs used here have a narrow size distribution with 20 nm mean diameter.[26] The proposed strategy involves the preparation of two samples for each molecule of interest, namely one in the presence of SNPs and the other without. By measuring the difference of ^{13}C NMR transverse spin relaxation in both types of samples, their SNP-interaction strengths can then be quantitatively determined and used to characterize the effect of the degree of *N*-methylation.[11]

We first assessed the dependence of the silica-binding affinity on the degree of *N*-methylation by selecting a cohort of molecules as model compounds, namely glycine (GLY), *N*-methylglycine, also known as sarcosine (SAR), *N*,*N*-dimethylglycine (DMG), and *N*,*N*,*N*-

trimethyl glycine (TMG, also known as betaine). They share the same molecular skeleton and only vary in the number of methyl groups directly attached to the same nitrogen atom, which can be 0, 1, 2, or 3. At neutral pH (7.0 ± 0.1) and the same ionic strength (20 mM sodium phosphate buffer), these compounds existed almost exclusively in their zwitterionic forms (see Table S1 in the Supporting Information (SI) for their pK_a values), displaying a negative charge on the deprotonated carboxyl group and a positive charge on the protonated amine or the quaternary ammonium. Therefore, the affinity changes observed here for different degrees of *N*-methylation are not due to changes in electrostatic attraction.

In the absence of SNPs, 1D ^{1}H NMR resonances of the methylene (–CH_2–) groups of all four compounds in aqueous solution (at 2.0 mM concentration each) have very similar intensities and linewidths. By contrast, the addition of SNPs (to 0.84 μM final SNP concentration) generates a differential line-broadening effect, from weakest for GLY to strongest for TMG, which rather nicely follows the degree of *N*-methylation (Figure 1A). Importantly, line-broadening and the absence of changes in resonance positions observed here, which is indicative of fast exchange dynamics, is consistent with previous findings for SNP interactions with free amino acids,[11] intrinsically disordered polypeptides,[39-40] and globular proteins.[41-42]

To accurately quantify the binding strength, we measured the ^{13}C NMR transverse relaxation rates (R_2) for the same set of samples using a ^{1}H-^{13}C HSQC-based proton-decoupled CPMG pulse sequence at ^{13}C natural abundance (1.1%). The difference of R_2 rates for each ^{13}C in the presence and absence of SNPs, denoted as ΔR_2, serves as a site-specific and highly sensitive measure of the fraction or population of molecules adsorbed to the surface of nanoparticles. From a microscopic point of view, a molecule interacting with a SNP via a specific group of atoms, leads to a reduction of its overall molecular tumbling thereby expediting

R_2 relaxation (Figure 1B). It can be shown that $\Delta R_2 \cong p_b R_2^b$ where R_2^b (>1000 s^{-1}) is the transverse relaxation rate of a ^{13}C spin rigidly anchored on the surface of a 20 nm spherical SNP, provided that the exchange rate constant k_{ex} fulfills $1/\tau_P >> k_{ex} >> R_2^b$ where τ_P is the tumbling correlation time of the free molecule. p_b is the SNP-bound population and R_2^b can be estimated from the Stokes-Einstein-Debye relationship (see SI).[11] p_b can thus be directly determined from $p_b \cong \Delta R_2 / R_2^b$, where ΔR_2 is the experimental differential transverse relaxation rate. Application to GLY, SAR, DMG, and TMG yields ΔR_2 values of 0.16, 0.76, 2.47, and 6.28 s^{-1}, respectively (Table 1), which means that the bound population of TMG is about 2.5-fold higher than that of DMG and 8-fold higher than SAR, whereas GLY barely interacts with silica. This trend is fully corroborated by the ^{13}C-ΔR_2 values of the methyl ($-CH_3$) carbons (Table 1). Consistent with the orthogonal and more qualitative information from ^1H NMR spectra (Figure 1A), it clearly shows the silicaphilic effect of the *N*-methyl motif.

For a more quantitative understanding of the binding behavior of molecules *X* to a nanoparticle *P*, we assume that each nanoparticle has a total of *N* distinct binding sites to which molecules *X* can bind independently with an association constant *K* in a non-cooperative fashion. Hence, a nanoparticle *P* can adopt states *P*, *PX*, PX_2, …, PX_N where state PX_n can be realized in $\binom{N}{n}$ possible ways. The concentrations of the different states of *P* can then be expressed as:

$$\begin{aligned} P + X &\Leftrightarrow PX & \left[PX\right] &= NK \cdot \left[P\right] \cdot \left[X\right] \\ P + 2X &\Leftrightarrow PX_2 & \left[PX_2\right] &= \binom{N}{2} K^2 \cdot \left[X\right]^2 \left[P\right] \\ &\cdots & &\cdots \\ P + N \cdot X &\Leftrightarrow PX_N & \left[PX_N\right] &= K^N \cdot \left[X\right]^N \left[P\right] \end{aligned} \qquad (1)$$

The bound population of *X* is then

$$p_b = p_{X,bound} = \left[X\right]_{bound} \Big/ \left[X\right]_{tot} = \left[X\right]_{bound} \Big/ \left(\left[X\right] + \left[X\right]_{bound}\right)$$

$$= \frac{\sum_{n=1}^{N} n \binom{N}{n} (Kx)^n \left[P\right]}{x + \sum_{n=1}^{N} n \binom{N}{n} (Kx)^n \left[P\right]} \approx \sum_{n=1}^{N} n \binom{N}{n} K^n x^{n-1} \left[P\right] \approx N \cdot K \cdot \left[P\right] \qquad (2)$$

where on the last line of Eq. (2) $x = [X] \approx [X]_{\text{free}} >> [X]_{\text{bound}}$ and $K \cdot x << 1$ were assumed. It shows that the bound population p_b is proportional to both the free nanoparticle concentration, the number of binding sites N, and equilibrium constant K. It follows for the ratio of the association constants of two different types of molecules X and Y under the assumption that the number of binding sites N per nanoparticle is the same:

$$\frac{K_X}{K_Y} = \frac{p_{b,X}}{p_{b,Y}} = \frac{\Delta R_{2,X}}{\Delta R_{2,Y}} \qquad (3)$$

Since only the population ratio enters Eq. (3), K_X/K_Y is independent of both R_2^b and N. From

$$K_X = \exp\{-\Delta G_{PX} / RT\} \qquad (4)$$

follows

$$\Delta\Delta G_{PX-PY} = -RT \ln \frac{p_{b,X}}{p_{b,Y}} = \Delta G_{PX} - \Delta G_{PY} \qquad (5)$$

where $\Delta\Delta G_{PX}$ is the free energy difference between the nanoparticle-bound and free state, R is the gas constant, and T is the absolute temperature. Eq. (5) allows the determination of the contribution of ligand modification, such as the addition of an *N*-methyl group, to the free energy of nanoparticle binding. Table 2 shows the results of the application of Eq. (5) to the experimental NMR data of GLY, SAR, DMG, and TMG. The addition of an *N*-methyl group to GLY has the largest effect on strengthening SNP affinity (–3.87 kJ/mol), whereas subsequent additions of *N*-methyl groups have a slightly smaller effect (–2.93 and –2.28 kJ/mol) with an average of –3.03 ± 0.80 kJ/mol per *N*-methyl group. The results show that the effect from multiple methyl groups is sizeable and in first order approximation additive allowing a maximal change of $\Delta\Delta G$ = –9.10 kJ/mol from GLY to TMG.

Next, we applied the same ^{13}C spin relaxation approach to a total of 13 RNA nucleosides and their methylated derivatives as well as to N^6-methyladenosine-5'-monophosphate (m^6AMP). They essentially cover the complete collection of naturally occurring forms of nucleobase methylation found in RNA. Samples were prepared at 12 ± 1 mM compound concentration, either with or without the presence of 3.36 μM SNPs (see SI). A broad range of ΔR_2 values were observed for these compounds, which are summarized in Figure 2 and SI, highlighting their variable binding affinities to silica surface.

Basic nucleosides in their native (non-methylated) forms, encompassing adenosine (A), guanosine (G), cytidine (C), uridine (U) and inosine (I, commonly found in tRNA), all have very limited interaction propensity with SNP surfaces ($\Delta R_2 < 3$ s^{-1}). In sharp contrast, the *N*-methylated forms of these nucleosides all manifest significant and systematic increase in their ΔR_2 values, indicative of elevated binding affinity. Among these compounds, 1-methyladenosine (m^1A), N^7-methylguanosine (m^7G), and N^3-methylcytosine (m^3C) fall into the same category

because the covalently bonded methyl groups change their net charge from 0 to +1. Considering that their ΔR_2 values are among the largest (Figure 2), this can be attributed, at least in part, to the prominent role of electrostatic attraction towards the negatively charged SNP surface.

By contrast, for N^6-methyladenosine (m^6A), N^6,N^6-dimethyladenosine ($m^6{}_2A$), and 4-methylcytidine (m^4C), which bear a net charge of 0, charge-charge Coulomb interactions can be excluded as the driving force for their interactions with SNPs. Still, all three compounds display considerable affinity to silica surfaces, which we attribute to the mere presence of the *N*-methyl motif. Averaged ΔR_2 values over all resolved carbon sites also reveal the systematic increase in the silica-binding affinities for A (average ΔR_2 = 1.4 s^{-1}), m^6A (5.5 s^{-1}), and $m^6{}_2A$ (13.8 s^{-1}), which reflects the cumulative effect from multiple *N*-methyl groups similar to GLY, SAR, DMG, and TMG. Analogous effects were also detected for DNA nucleosides, as exemplified by the increased silica affinity of N^6-methyl-2'-deoxyadenosine (m^6dA, average ΔR_2 = 18.3 s^{-1}) compared to its unmodified counterpart (4.4 s^{-1}).

Addition of an *N*-methyl group has a mean binding free energy $\Delta\Delta G$, according to Eq. (5), for the neutral m^6A/A, $m^6{}_2A$/m^6A, m^4C/C, m^6dA/dA, and N^3-methylyridine (m^3U)/U pairs of –3.05 ± 0.50 kJ/mol. This value is remarkably close to those of GLY, SAR, DMG, and TMG of –3.03 ± 0.80 kJ/mol (Table S2). Hence, the mean free energy gain for pristine silica-surface binding per *N*-methyl group in the absence of change of net charge is $\Delta\Delta G$ = –3.04 ± 0.57 kJ/mol. In the case of m^3U vs. U, the ΔR_2 values are considerably smaller in absolute terms, but the fold change of the bound population is fully consistent with the rest of the molecules. The low silica affinity of m^3U/U may be a consequence of the two ketones flanking the nitrogen atom and their strong solvation propensity in water counteracting the surface-binding tendency of the *N*-methyl motif. Reduced affinity is also observed for 5-methyluridine (m^5U) where methylation

occurs at a carbon rather than a nitrogen site (Table S2). Clearly, the effect of C-methylation on nanoparticle binding deserves further investigations using the methods described here.

The site-specific methylation in m^1A, m^7G, and m^3C alters the net molecular charge from 0 to +1 with respect to their parent molecules A, G, and C leading to significantly larger $\Delta\Delta G$ values of –8.43, –9.08, and –6.19 kJ/mol, respectively. Compared to –3.04 kJ/mol found for *N*-methylation without charge change, the combined contributions of electrostatic attraction and possibly other interactions are directly revealed. Likewise, when comparing m^6AMP (average $\Delta R_2 = 1.5\ s^{-1}$) to m^6A ($5.6\ s^{-1}$), the reduced silica-binding affinity with a $\Delta\Delta G = +3.26$ kJ/mol can be largely attributed to electrostatic repulsion with respect to the anionic silica surface due to its –2 net charge state. We conclude that the *N*-methyl motif has a strong silicaphilic propensity and enhances molecular binding to pristine silica surfaces, while at the same time other driving forces, especially electrostatics, contribute to the interaction strengths in either a synergistic or an opposing manner. These findings should help the design of new molecules with targeted binding free energies to SNP surfaces.

Strong evidence has emerged of the widespread functional role of *N*-methylation in biological molecules, including DNA, RNA, and proteins.[43-44] However, their mode of interaction with the surroundings has remained largely open. Due to their bulkiness, *N*-methyl groups can introduce local steric hinderance. For example, in the case of m^6A, it favors single over double-stranded stranded RNA making the RNA better accessible to protein recognition.[45-46] By changing the local chemical properties, methylation has also a profound effect on the interaction strength with binding partners as has been quantitatively demonstrated by ^{13}C NMR spin relaxation for the case of SNPs.

The NMR relaxation method fulfills a clear need as a versatile experimental approach that is sensitive to weak and dynamic binding events providing such information throughout different parts of a molecule. The method can be applied to an extraordinary wide range of molecules containing CH, CH_2, or CH_3 groups and is thereby not limited, for example, to systems with specific optical properties. It can also be used to investigate molecules interacting with other large surface structures that can have a biological or synthetic origin, including large proteins, nucleic acids or membranes, and other types of nanoparticles and other nanostructures. When experimental conditions such as temperature, concentration, and pH are carefully controlled, the ΔR_2 values provide quantitative bound population information, as shown here, making direct comparisons among different molecules possible for the extraction of binding free energy differences. The site-resolved ΔR_2 values even offer a glimpse of intramolecular binding orientations and points of contact. In particular, atoms that preferentially make direct contact with the SNP surface have larger ΔR_2 values, whereas atoms that are flexibly linked to the primary atom contacts and are on average further away from the surface can undergo tethering, thereby experiencing a decrease in ΔR_2. For example, the ribose rings of RNA nucleosides generally have a smaller ΔR_2 than ^{13}C atoms of the base (Table S3), suggesting that the ribose undergoes tethering whereas the nucleobases directly interact with the nanoparticle surface. The conversion of the NMR relaxation data to $\Delta\Delta G$ values assumes that the dynamics of the bound states of molecules is independent of their methylation state. Recently, NMR ΔR_2 were was used together with ^{13}C-DEST to model the global dynamics of phenol when bound to ceria nanoparticle catalysts.[17,47]

In summary, it has been demonstrated by quantitative NMR spin relaxation how *N*-methylation significantly promotes the silicaphilic propensity of metabolites. Remarkably, of

nearly two dozen molecules studied here we did not encounter a single violation to this behavior. We find that the trimethylated forms have the strongest affinity, followed by dimethylated and monomethylated forms. This empirical rule helps both simplify and quantify our understanding of adsorption of this class of compounds to silica surfaces, which can guide the design and synthesis[48-49] of new molecules with predefined nanoparticle affinities by shifting the equilibrium from mostly free molecules to higher population bound states. These rules can also find fruitful applications for nanoparticle-assisted metabolomics[50] or the separation of nucleic acid samples *in vitro* based on their degree of methylation.[51] In the long term, it may be even feasible to generalize and adapt the binding properties of nucleic acids methylated at specific positions,[52] including the ones characterized here, for the regulation of biological pathways *in vivo* to control the recognition between nucleosides and enzymes, receptors, membranes, and their assemblies, in their native biological environment.

Figures and Tables

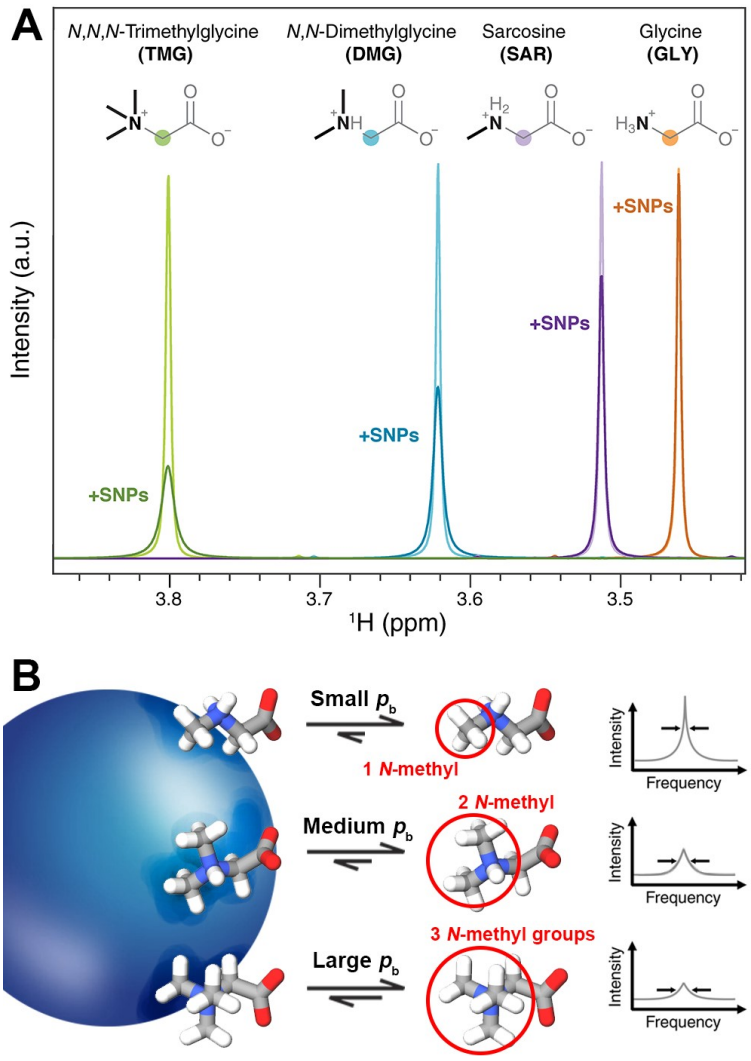

Figure 1. (A) Effect of degree of *N*-methylation of GLY to SAR, DMG, and TMG on their interaction propensities with silica nanoparticles. Superposition of experimental ^{1}H NMR spectra of the $-CH_2-$ proton resonances of the four compounds in the presence (darker colors) and absence (lighter colors) of SNPs shows differential dependence of spectral line-broadening accompanied by a decrease of peak amplitudes, which directly reflect the binding affinity on the degree of *N*-methylation. (B) Illustration of the measurement of the bound population, p_b, of molecules with different degrees of *N*-methylation to silica nanoparticles by solution NMR transverse spin relaxation. Molecules that transiently interact with silica nanoparticles (large blue sphere) experience faster transverse NMR spin relaxation, causing a larger linewidth that can be accurately measured as an effective relaxation rate and compared with the corresponding relaxation rate in the absence of nanoparticles (see main text and SI).

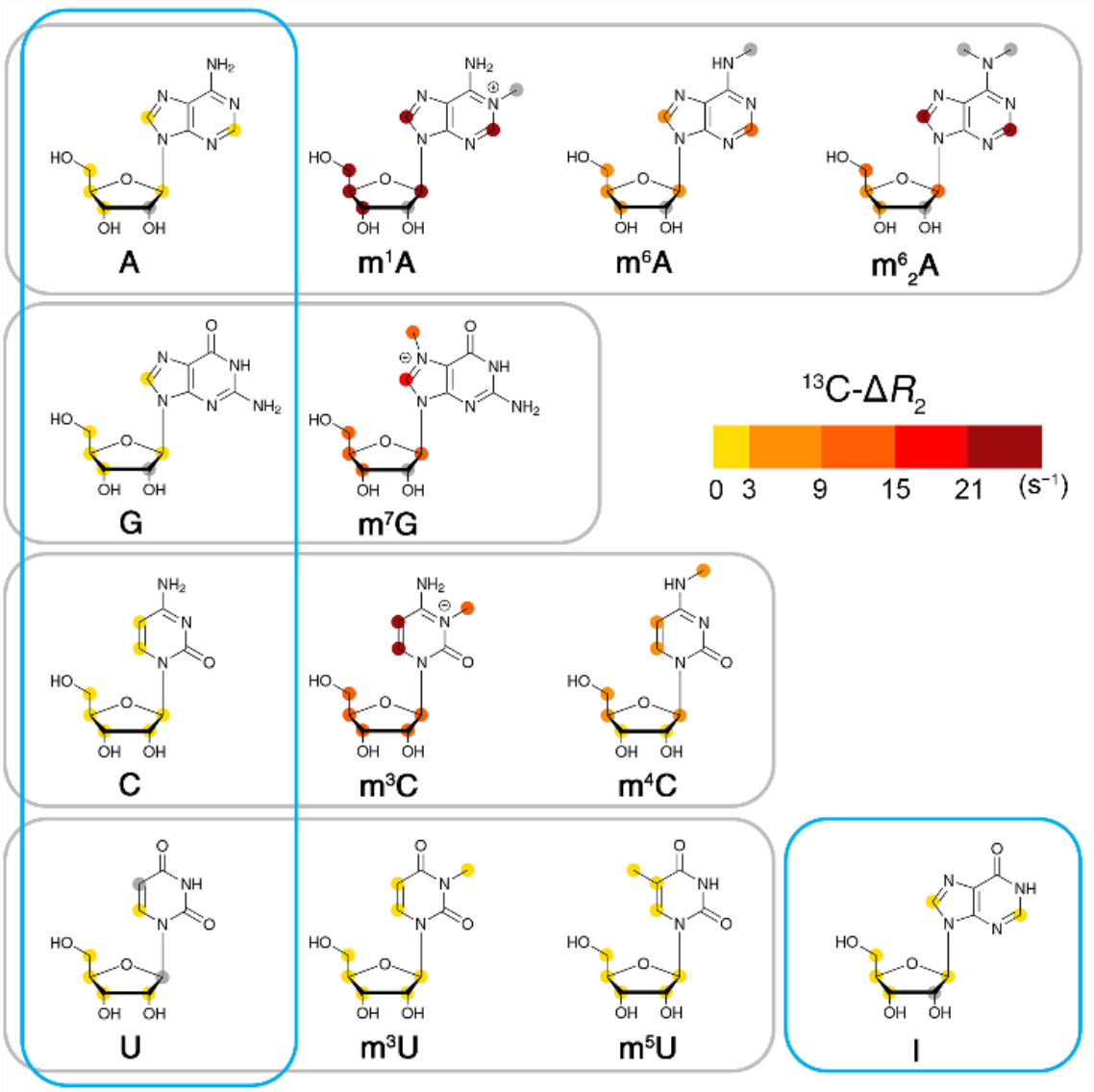

Figure 2. Mapping of experimentally determined site-specific differences, ΔR_2, of ^{13}C-R_2 spin relaxation rates in the presence and absence of SNPs on the structures of 13 different RNA nucleosides. The absolute ΔR_2 values, which are a measure of the change in binding affinity (Eqs. (3), (S4)), are depicted as color-coded solid circles, from very low (yellow, weak binding) to high (dark red, strong binding) values. Gray circles indicate that the corresponding carbon resonance either disappeared due to rapid relaxation (e.g. methyl groups of m^1A, m^6A, and $m^6{}_2A$) or overlapped with other resonances (including water) and thus could not be accurately quantified. Nucleosides grouped together inside a gray box share the same nucleobase, and blue boxes highlight nucleosides in their non-methylated forms.

Table 1. Enhanced methylene and methyl ^{13}C-R_2 spin relaxation of GLY, SAR, DMG, and TMG via interactions with silica nanoparticles.

Compound	Methylene –CH_2– ^{13}C-R_2 (s^{-1}) [a]			Methyl –CH_3 ^{13}C-R_2 (s^{-1}) [a]		
	no SNPs	with SNPs	ΔR_2	no SNPs	with SNPs	ΔR_2
GLY	0.63	0.79	**0.16** ± 0.04	-	-	-
SAR	1.42	2.18	**0.76** ± 0.23	1.59	2.04	**0.45** ± 0.08
DMG	0.90	3.37	**2.47** ± 0.28	0.79	2.94	**2.15** ± 0.08
TMG	0.54	6.82	**6.28** ± 0.23	0.52	4.14	**3.63** ± 0.16

[a] Errors estimated by error propagation are only reported for ΔR_2.

Table 2. Effect of *N*-methyl group additions on nanoparticle binding of GLY, SAR, DMG, and TMG expressed as free energy changes $\Delta\Delta G_{PX\text{-}PY}$ (kJ/mol)

$\Delta\Delta G$ (kJ/mol)	**GLY (0)** [a]	**SAR (1)**	**DMG (2)**	**TMG (3)**
GLY (0) [a]	0	3.87	6.87	9.10
SAR (1)	–3.87	0	2.93	5.23
DMG (2)	–6.87	–2.93	0	2.28
TMG (3)	–9.10	–5.23	–2.28	0

[a] The numbers in parentheses indicate the number of *N*-methyl groups attached to the nitrogen.

ASSOCIATED CONTENT

Acknowledgement. This work was supported by the U.S. National Science Foundation (grant MCB-1715505) and the National Institutes of Health (grant GM066041). We thank Dr. Lei Bruschweiler-Li and Dr. Alexandar Hansen for their expert help. All NMR experiments were performed at the CCIC NMR facility at The Ohio State University.

Supporting Information. The following files are available free of charge. Further details of the materials and methods, calculations, and tables with experimental data (PDF); experimental R_2 data of nucleosides (Excel).

Notes

The authors declare no competing financial interests.

REFERENCES

(1) Wang, L.; Zhao, W.; Tan, W., Bioconjugated Silica Nanoparticles: Development and Applications. *Nano Res.* **2008**, *1*, 99-115.

(2) Qian, K.; Yang, Z.; Zhang, F.; Yang, B.; Dasgupta, P. K., Low-Bleed Silica-Based Stationary Phase for Hydrophilic Interaction Liquid Chromatography. *Anal. Chem.* **2018**, *90*, 8750-8755.

(3) Liang, J.; Liang, Z.; Zou, R.; Zhao, Y., Heterogeneous Catalysis in Zeolites, Mesoporous Silica, and Metal–Organic Frameworks. *Adv. Mater.* **2017**, *29*, 1701139.

(4) Van den Bergh, M.; Krajnc, A.; Voorspoels, S.; Tavares, S. R.; Mullens, S.; Beurroies, I.; Maurin, G.; Mali, G.; De Vos, D., Highly Selective Removal of Perfluorinated Contaminants by Adsorption on All-Silica Zeolite Beta. *Angew. Chem. Int. Ed.* **2020**, *59*, 14086-14090.

(5) Capeletti, L. B.; Loiola, L. M.; Picco, A. S.; da Silva Liberato, M.; Cardoso, M. B., Silica Nanoparticle Applications in the Biomedical Field. In *Smart Nanoparticles for Biomedicine*, Elsevier: 2018; pp 115-129.

(6) Wen, J.; Yang, K.; Liu, F.; Li, H.; Xu, Y.; Sun, S., Diverse Gatekeepers for Mesoporous Silica Nanoparticle Based Drug Delivery Systems. *Chem. Soc. Rev.* **2017**, *46*, 6024-6045.

(7) Schrader, A. M.; Monroe, J. I.; Sheil, R.; Dobbs, H. A.; Keller, T. J.; Li, Y.; Jain, S.; Shell, M. S.; Israelachvili, J. N.; Han, S., Surface Chemical Heterogeneity Modulates Silica Surface Hydration. *Proc. Natl. Acad. Sci. U.S.A.* **2018**, *115*, 2890-2895.

(8) Li, J.; Luo, J., Nonlinear Frictional Energy Dissipation between Silica-Adsorbed Surfactant Micelles. *J. Phys. Chem. Lett.* **2017**, *8*, 2258-2262.

(9) Parida, S. K.; Dash, S.; Patel, S.; Mishra, B., Adsorption of Organic Molecules on Silica Surface. *Adv. Colloid Interface Sci.* **2006**, *121*, 77-110.

(10) Sato, N.; Aoyama, Y.; Yamanaka, J.; Toyotama, A.; Okuzono, T., Particle Adsorption on Hydrogel Surfaces in Aqueous Media Due to van der Waals Attraction. *Sci. Rep.* **2017**, *7*, 1-10.

(11) Xie, M.; Hansen, A. L.; Yuan, J.; Brüschweiler, R., Residue-Specific Interactions of an Intrinsically Disordered Protein with Silica Nanoparticles and Their Quantitative Prediction. *J. Phys. Chem. C* **2016**, *120*, 24463-24468.

(12) Thibaut, A.; Misselyn-Bauduin, A.-M.; Grandjean, J.; Broze, G.; Jérôme, R., Adsorption of an Aqueous Mixture of Surfactants on Silica. *Langmuir* **2000**, *16*, 9192-9198.

(13) Xiong, Y.; Li, Z.; Cao, T.; Xu, S.; Yuan, S.; Sjöblom, J.; Xu, Z., Synergistic Adsorption of Polyaromatic Compounds on Silica Surfaces Studied by Molecular Dynamics Simulation. *J. Phys. Chem. C* **2018**, *122*, 4290-4299.

(14) Plekan, O.; Feyer, V.; Šutara, F.; Skála, T.; Švec, M.; Cháb, V.; Matolín, V.; Prince, K., The Adsorption of Adenine on Mineral Surfaces: Iron Pyrite and Silicon Dioxide. *Surf. Sci.* **2007**, *601*, 1973-1980.

(15) Bergna, H. E.; Roberts, W. O., *Colloidal Silica: Fundamentals and Applications*; CRC Press, 2005; Vol. 131.

(16) Diez-Castellnou, M.; Salvia, M. V.; Springhetti, S.; Rastrelli, F.; Mancin, F., Nanoparticle-Assisted Affinity NMR Spectroscopy: High Sensitivity Detection and Identification of Organic Molecules. *Chem.-Eur. J.* **2016**, *22*, 16957-16963.

(17) Egner, T. K.; Naik, P.; Nelson, N. C.; Slowing, I. I.; Venditti, V., Mechanistic Insight into Nanoparticle Surface Adsorption by Solution NMR Spectroscopy in an Aqueous Gel. *Angew. Chem. Int. Ed.* **2017**, *56*, 9802-9806.

(18) Zhang, Y.; Casabianca, L. B., Probing Amino Acid Interaction with a Polystyrene Nanoparticle Surface Using Saturation-Transfer Difference (STD)-NMR. *J. Phys. Chem. Lett.* **2018**, *9*, 6921-6925.

(19) Young, G., Interaction of Water Vapor with Silica Surfaces. *J. Colloid Sci.* **1958**, *13*, 67-85.

(20) Bowen, T. C.; Vane, L. M., Ethanol, Acetic Acid, and Water Adsorption from Binary and Ternary Liquid Mixtures on High-Silica Zeolites. *Langmuir* **2006**, *22*, 3721-3727.

(21) Sanz-Pérez, E.; Dantas, T.; Arencibia, A.; Calleja, G.; Guedes, A.; Araujo, A.; Sanz, R., Reuse and Recycling of Amine-Functionalized Silica Materials for CO2 Adsorption. *Chem. Eng. J.* **2017**, *308*, 1021-1033.

(22) Minju, N.; Nair, B. N.; Mohamed, A. P.; Ananthakumar, S., Surface Engineered Silica Mesospheres–a Promising Adsorbent for CO2 Capture. *Sep. Purif. Techol.* **2017**, *181*, 192-200.

(23) Abelard, J.; Wilmsmeyer, A. R.; Edwards, A. C.; Gordon, W. O.; Durke, E. M.; Karwacki, C. J.; Troya, D.; Morris, J. R., Adsorption of Substituted Benzene Derivatives on Silica: Effects of Electron Withdrawing and Donating Groups. *J. Phys. Chem. C* **2016**, *120*, 13024-13031.

(24) Remesal, E. R.; Amaya, J.; Graciani, J.; Marquez, A. M.; Sanz, J. F., Adsorption of Prototypical Amino Acids on Silica: Influence of the Pre-Adsorbed Water Multilayer. *Surf. Sci.* **2016**, *646*, 239-246.

(25) Rimola, A.; Costa, D.; Sodupe, M.; Lambert, J.-F.; Ugliengo, P., Silica Surface Features and Their Role in the Adsorption of Biomolecules: Computational Modeling and Experiments. *Chem. Rev.* **2013**, *113*, 4216-4313.

(26) Zhang, B.; Xie, M.; Bruschweiler-Li, L.; Bingol, K.; Brüschweiler, R., Use of Charged Nanoparticles in Nmr-Based Metabolomics for Spectral Simplification and Improved Metabolite Identification. *Anal. Chem.* **2015**, *87*, 7211-7217.

(27) Zhang, B.; Xie, M.; Bruschweiler-Li, L.; Brüschweiler, R., Nanoparticle-Assisted Removal of Protein in Human Serum for Metabolomics Studies. *Anal. Chem.* **2016**, *88*, 1003-1007.

(28) Xiang, Y.; Laurent, B.; Hsu, C.-H.; Nachtergaele, S.; Lu, Z.; Sheng, W.; Xu, C.; Chen, H.; Ouyang, J.; Wang, S., RNA m6A Methylation Regulates the Ultraviolet-Induced DNA Damage Response. *Nature* **2017**, *543*, 573-576.

(29) Novik, K.; Nimmrich, I.; Genc, B.; Maier, S.; Piepenbrock, C.; Olek, A.; Beck, S., Epigenomics: Genome-Wide Study of Methylation Phenomena. *Curr. Issues. Mol. Biol.* **2002**, *4*, 111-128.

(30) Jia, G.; Fu, Y.; He, C., Reversible Rna Adenosine Methylation in Biological Regulation. *Trends Genet.* **2013**, *29*, 108-115.

(31) Motorin, Y.; Helm, M., RNA Nucleotide Methylation. *Wiley Interdiscip. Rev. RNA* **2011**, *2*, 611-631.

(32) Fu, Y.; Jia, G.; Pang, X.; Wang, R. N.; Wang, X.; Li, C. J.; Smemo, S.; Dai, Q.; Bailey, K. A.; Nobrega, M. A., FTO-Mediated Formation of N6-Hydroxymethyladenosine and N6-Formyladenosine in Mammalian RNA. *Nat. Commun.* **2013**, *4*, 1-8.

(33) Squires, J. E.; Patel, H. R.; Nousch, M.; Sibbritt, T.; Humphreys, D. T.; Parker, B. J.; Suter, C. M.; Preiss, T., Widespread Occurrence of 5-Methylcytosine in Human Coding and Non-Coding RNA. *Nucleic Acids Res.* **2012**, *40*, 5023-5033.

(34) Chen, Y. G.; Kowtoniuk, W. E.; Agarwal, I.; Shen, Y.; Liu, D. R., LC/MS Analysis of Cellular RNA Reveals NAD-Linked RNA. *Nat. Chem. Biol.* **2009**, *5*, 879.

(35) Marchand, V.; Ayadi, L.; Ernst, F. G.; Hertler, J.; Bourguignon-Igel, V.; Galvanin, A.; Kotter, A.; Helm, M.; Lafontaine, D. L.; Motorin, Y., Alkaniline-Seq: Profiling of m7G and m3C RNA Modifications at Single Nucleotide Resolution. *Angew. Chem. Int. Ed.* **2018**, *57*, 16785-16790.

(36) Dominissini, D.; Nachtergaele, S.; Moshitch-Moshkovitz, S.; Peer, E.; Kol, N.; Ben-Haim, M. S.; Dai, Q.; Di Segni, A.; Salmon-Divon, M.; Clark, W. C., The Dynamic N1-Methyladenosine Methylome in Eukaryotic Messenger RNA. *Nature* **2016**, *530*, 441-446.

(37) Pérez, A.; Castellazzi, C. L.; Battistini, F.; Collinet, K.; Flores, O.; Deniz, O.; Ruiz, M. L.; Torrents, D.; Eritja, R.; Soler-López, M., Impact of Methylation on the Physical Properties of DNA. *Biophys. J.* **2012**, *102*, 2140-2148.

(38) Luo, S.; Tong, L., Molecular Basis for the Recognition of Methylated Adenines in RNA by the Eukaryotic YTH Domain. *Proc. Natl. Acad. Sci. U.S.A.* **2014**, *111*, 13834-13839.

(39) Xie, M.; Li, D. W.; Yuan, J.; Hansen, A. L.; Brüschweiler, R., Quantitative Binding Behavior of Intrinsically Disordered Proteins to Nanoparticle Surfaces at Individual Residue Level. *Chem.-Eur. J.* **2018**, *24*, 16997-17001.

(40) Li, D.-W.; Xie, M.; Brüschweiler, R., Quantitative Cooperative Binding Model for Intrinsically Disordered Proteins Interacting with Nanomaterials. *J. Am. Chem. Soc.* **2020**, *142*, 10730-10738.

(41) Xie, M.; Yu, L.; Bruschweiler-Li, L.; Xiang, X.; Hansen, A. L.; Brüschweiler, R., Functional Protein Dynamics on Uncharted Time Scales Detected by Nanoparticle-Assisted NMR Spin Relaxation. *Sci. Adv.* **2019**, *5*, eaax5560.

(42) Wardenfelt, S.; Xiang, X.; Xie, M.; Yu, L.; Bruschweiler-Li, L.; Brüschweiler, R., Broadband Dynamics of Ubiquitin by Anionic and Cationic Nanoparticle-Assisted NMR Spin Relaxation. *Angew. Chem. Int. Ed.* **2020**, Sep 9. DOI: 10.1002/anie.202007205.

(43) Chatterjee, J.; Rechenmacher, F.; Kessler, H., N-Methylation of Peptides and Proteins: An Important Element for Modulating Biological Functions. *Angew. Chem. Int. Ed.* **2013**, *52*, 254-269.

(44) Roundtree, I. A.; Evans, M. E.; Pan, T.; He, C., Dynamic RNA Modifications in Gene Expression Regulation. *Cell* **2017**, *169*, 1187-1200.

(45) Roost, C.; Lynch, S. R.; Batista, P. J.; Qu, K.; Chang, H. Y.; Kool, E. T., Structure and Thermodynamics of N6-Methyladenosine in RNA: A Spring-Loaded Base Modification. *J. Am. Chem. Soc.* **2015**, *137*, 2107-2115.

(46) Shi, H.; Liu, B.; Nussbaumer, F.; Rangadurai, A.; Kreutz, C.; Al-Hashimi, H. M., NMR Chemical Exchange Measurements Reveal That N6-Methyladenosine Slows RNA Annealing. *J. Am. Chem. Soc.* **2019**, *141*, 19988-19993.

(47) Egner, T.; Naik, P.; An, Y.; Venkatesh, A.; Rossini, A.; Slowing, I.; Venditti, V. 'Surface Contrast' NMR Reveals Non-Innocent Role of Support in Pd/CeO_2 Catalyzed Phenol Hydrogenation. *ChemCatChem*. **2020**, *12*, 4160-4166.

(48) Cabrero-Antonino, J. R.; Adam, R.; Junge, K.; Beller, M. A General Protocol for the Reductive N-Methylation of Amines Using Dimethyl Carbonate and Molecular Hydrogen: Mechanistic Insights and Kinetic Studies. *Catal. Sci. Technol.* **2016**, *6*, 7956-7966.

(49) Tsarev, V. N.; Morioka, Y.; Caner, J.; Wang, Q.; Ushimaru, R.; Kudo, A.; Naka, H.; Saito, S. (2015). N-Methylation of Amines with Methanol at Room Temperature. *Org. Lett.* **2015,** *17*, 2530-2533.

(50) Zhang, B.; Xie, M.; Bruschweiler-Li, L.; Brüschweiler, R., Nanoparticle-Assisted Metabolomics. *Metabolites* **2018**, *8*, 21.

(51) Poeckh, T.; Lopez, S.; Fuller, A. O.; Solomon, M. J.; Larson, R. G., Adsorption and Elution Characteristics of Nucleic Acids on Silica Surfaces and Their Use in Designing a Miniaturized Purification Unit. *Anal. Biochem.* **2008**, *373*, 253-262.

(52) Gedda, M. R.; Babele, P. K.; Zahra, K.; Madhukar, P., Epigenetic Aspects of Engineered Nanomaterials: Is the Collateral Damage Inevitable? *Front. Bioeng. Biotech.* **2019**, *7*: 228.